PAPER

Check for updates

Degradation of azo dye with activated peroxygens: when zero-valent iron meets chloride†

Zhaohui Wang, [ID] *[ab] Luoyan Ai,[a] Ying Huang,[a] Juekai Zhang,[ac] Sitong Li,[ac] Jiawei Chen[ac] and Fei Yang[a]

Degradation of acid orange 7 (AO7) by Fe^0-based Advance Oxidation Process (AOPs) with common peroxygens, persulfate (PS), peroxymonosulfate (PMS) and hydrogen peroxide (H_2O_2), was investigated, in which sulfate radicals ($SO_4^{\cdot-}$) and/or hydroxyl radicals ($^{\cdot}OH$) are powerful oxidizing species. The effects of Fe^0 dosage, peroxygen concentration, initial pH and the presence of chloride on the degradation of AO7 were examined. The AO7 degradation efficiencies by four systems, including Fe^0, Fe^0/H_2O_2, Fe^0/PMS and Fe^0/PS were compared. AO7 degradation rate by Fe^0 activated AOPs in descending order is $H_2O_2 \geqq PS > PMS$. Increasing acidity and iron dosage favored a rapid degradation of AO7. The presence of chloride greatly inhibited dye removal in Fe^0/H_2O_2 and Fe^0/PS systems, whilst accelerated dye degradation was observed in the Fe^0/PMS system. In contrast, mineralization of AO7 in the $Fe^0/PMS/Cl^-$ system was minimal, because of formation of lots of refractory chlorinated phenols as identified by GC–MS. These findings are useful for selecting the most appropriate technology for textile wastewater treatment, depending on the wastewater constituents and pH.
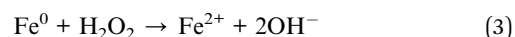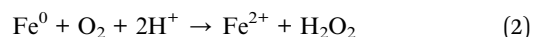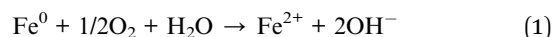
1. Introduction

It is reported that over 100 000 kinds of synthetic dyes are widely used in the textile, plastic, paper, food, cosmetic, pharmaceutical and photographic industries. An estimated 10–20% of dyes under production and in the dyeing process are discharged to the environment.[1] Therefore, textile wastewater is one of the important industrial pollution sources in developing countries. Azo dyes are of great concern due to their extensive use, carcinogenesis and biorecalcitrance for traditional biological treatment technologies.[2] In consideration of the increasingly strict legislations and regulations, it is urgent for the associated industries to develop economically viable technology to remove azo dyes from industrial effluents.

Iron is one of the most abundant metals in the Earth's crust. In recent years, zero-valent iron (ZVI) has been extensively applied to environmental remediation because of its ability to reduce organic pollutants, such as, chlorinated solvents, polychlorobiphenyls (PCBs), pesticides and dyes under anoxic conditions.[3–11] More recently, several investigations have

[a]*State Environmental Protection Engineering Center for Pollution Treatment and Control in Textile Industry, College of Environmental Science and Engineering, Donghua University, Shanghai, 201620, China. E-mail: zhaohuiwang@dhu.edu.cn*

[b]*International Center for Balanced Land Use (ICBLU), The University of Newcastle, Callaghan, NSW 2308, Australia*

[c]*Shanghai Shixi High School (SSHS), Jing'an District, Shanghai, 200040, China*

† Electronic supplementary information (ESI) available: The online version of this article contains supplementary material, which is available to authorized users. See DOI: 10.1039/c7ra03872k

reported oxidation of ZVI with oxygen can lead to the formation of reactive oxygen species (ROS) capable of degrading pollutants that cannot be reduced by ZVI. Yields of ROS from oxygen activation with ZVI are significantly affected by pH.[12,13] Fe^0 or ferrous ions ($Fe(II)$) released from Fe^0 corrosion, react with oxygen to produce H_2O_2, which further reacts with $Fe(II)$ via a well-known Fenton reaction to produce $^{\cdot}OH$ (eqn (1)–(4)).[14–16]

$$Fe^0 + 1/2O_2 + H_2O \rightarrow Fe^{2+} + 2OH^- \tag{1}$$

$$Fe^0 + O_2 + 2H^+ \rightarrow Fe^{2+} + H_2O_2 \tag{2}$$

$$Fe^0 + H_2O_2 \rightarrow Fe^{2+} + 2OH^- \tag{3}$$

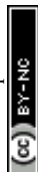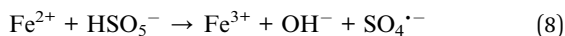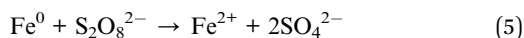$$Fe^{2+} + H_2O_2 \rightarrow Fe^{3+} + OH^- + {}^{\cdot}OH \tag{4}$$

In addition to oxygen, ZVI has been successfully used to activate a series of peroxygens like H_2O_2, persulfate (PS, $S_2O_8^{2-}$) and peroxymonosulfate (PMS, HSO_5^-).[17–21] Fe^0 is a strong electron donor ($E^0(Fe^{2+}/Fe^0) = -0.447$ V vs. NHE)[19] and is expected to induce reductive decomposition of H_2O_2 ($E^0(H_2O_2/H_2O) = 1.77$ V vs. NHE),[22] PS ($E^0(S_2O_8^{2-}/SO_4^{2-}) = 2.01$ V vs. NHE) and PMS ($E^0(HSO_5^-/HSO_4^-) = 1.85$ V vs. NHE)[23] (eqn (5) and (6)). ZVI is thought to act as a continuous slow-release source of $Fe(II)$ during peroxygens activation. The peroxo bond in these peroxygens breaks down by $Fe(II)$ to form highly reactive oxidants, such as $^{\cdot}OH$ and $SO_4^{\cdot-}$ (eqn (7) and (8)). Therefore, peroxygens activation with ZVI has been applied to degrade several contaminants such as aniline, bisphenol, trichloroethene, phenol, acid black 24 and pentachlorophenol.[17,24–28] To the best

of our knowledge, a comparative study on the degradation of the same azo dye by ZVI-based peroxygens activation has not been reported.

$$Fe^0 + S_2O_8{}^{2-} \rightarrow Fe^{2+} + 2SO_4{}^{2-} \tag{5}$$

$$Fe^0 + HSO_5{}^- \rightarrow Fe^{2+} + SO_4{}^{2-} + OH^- \tag{6}$$

$$Fe^{2+} + S_2O_8{}^{2-} \rightarrow Fe^{3+} + SO_4{}^{2-} + SO_4{}^{\cdot-} \tag{7}$$

$$Fe^{2+} + HSO_5{}^- \rightarrow Fe^{3+} + OH^- + SO_4{}^{\cdot-} \tag{8}$$

The present study was an attempt to compare the degradation efficiencies of Acid Orange 7 (AO7, a typical azo dye) by ZVI activation with three common peroxygens. The effects of pH, ZVI dosage, chloride ions on dye degradation were investigated. Additionally, TOC and GC-MS measurement were conducted to characterize the extent of mineralization and intermediate products during treatment.

2. Experimental

2.1. Materials

All chemical reagents used in this study were in AR grade and were used without further purification. Hydrogen peroxide (30%, v/v), sodium chloride (NaCl), sodium hydroxide (NaOH), sulfuric acid (H_2SO_4, 98%), and the Fe^0 powder were obtained from Sinopharm. Acid orange 7 ($C_{16}H_{11}N_2O_4SNa$) and Oxone® ($2KHSO_5 \cdot KHSO_4 \cdot K_2SO_4$) were bought from Sigma-Aldrich. Potassium persulfate ($K_2S_2O_8$) was purchased from Alfa Aesar. All solutions were prepared with deionized water.

2.2. Experimental procedures

The degradation experiments were conducted at room temperature in 250 mL batch reactors, and used the same batch reactors to make all comparisons. For all the experiments, the initial concentration of AO7 was 0.08 mmol L^{-1}. The initial pH values of all solutions were adjusted by 0.1 mol L^{-1} sulfuric acid or 0.1 mol L^{-1} sodium hydroxide. At given intervals, the solution was sampled and examined on U-2910 spectrophotometer at 484 nm for testing the degradation kinetics. For the measurement of mineralization and products, samples were quenched by sodium nitrite with a ratio of $NaNO_2$/react solution was 1 : 1. All experiments were conducted in duplicate.

2.3. Analysis

The analysis of the degradation intermediates was carried out by gas chromatography-mass spectrometry (Agilent 7890A model GC with DB-5 MS. 30 mm × 320 μm × 0.5 μm capillary column coupled with 5975A inert XL MSD model MS). Helium was used as the carrier gas at a rate of 1.0 mL min^{-1}. 1 μL samples were injected at 250 °C in splitless mode. The sequence of GC temperature program was followed as: start at 40 °C, hold for 2 min; 40–100 °C (12 °C min); 100–200 °C (5 °C min); 200–270 °C (20 °C min^{-1}), hold for 5 min. The ion source temperature was maintained at 230 °C. Qualitative detector was used in the electron impact (EI) mode at 70 eV with the mass scanned range (30–400 m/z). The unknown peaks were identified using NIST08 mass spectral library database.

The mineralization of AO7 aqueous solutions was examined by a Shimazu TOC-V_{CPH} analyzer. The sample volumes were 10 mL. The flow rate and pressure of carrying gas (air) was set as 150 mL min^{-1} and 300 kPa, respectively.

A pseudo first-order kinetic model is used to describe the degradation kinetics in different activation systems. The kinetic expression is represented as eqn (9), where C_t is the residual AO7 concentration at time t (min); C_0 is the initial AO7 concentration. k denotes the observed pseudo first-order rate

Table 1 The calculated pseudo first-order rate constant (10^{-3} min^{-1}) of AO7 oxidation in Fe^0-peroxygens systems

		Fe		Fe/H_2O_2		Fe/PMS		Fe/PS	
		k	R^2	k	R^2	k	R^2	k	R^2
pH[a]	2.5	6.5	0.983	160	0.978	120	0.930	120	0.982
	4.0	—	—	7.2	0.997	63	0.992	68	0.948
	7.0	—	—	—	—	28	0.998	5.3	0.995
Iron dosage (g L^{-1})[b]	0.005	2.1	0.913	59	0.950	74	0.999	26	0.998
	0.025	8.0	0.973	91	0.900	54	0.958	140	0.988
	0.1[c]	37	0.994	220	0.942	91	0.985	260	0.999
Peroxygens concentration (mmol L^{-1})[d]	0	—	—	6.4	0.984	7.6	0.988	8.2	0.999
	0.5	—	—	55	0.980	56	0.945	67	0.999
	1.0	—	—	96	0.940	81	0.906	130	0.994
	1.5	—	—	150	0.986	45	0.991	160	0.969
Cl^- concentration (mmol L^{-1})[e]	0	7.6	0.988	120	0.929	51	0.969	120	0.993
	50	7.6	0.996	100	0.992	140	0.911	92	0.964
	300	6.7	0.999	110	0.969	440	0.957	43	0.982
	400	5.7	0.999	150	0.986	780	0.978	44	0.984

[a] Conditions: $m(Fe^0)$ = 0.025 g L^{-1}, $c(Ox)$ = 1.0 mmol L^{-1}, $c(AO7)$ = 0.08 mmol L^{-1}. [b] Conditions: $c(Ox)$ = 1.0 mmol L^{-1}, $c(AO7)$ = 0.08 mmol L^{-1}, pH = 2.5. [c] Conditions: in Fe/PMS, the maximum dosage of Fe^0 was 0.05 g L^{-1}. [d] Conditions: $m(Fe^0)$ = 0.025 g L^{-1}, $c(AO7)$ = 0.08 mmol L^{-1}, pH = 2.5. [e] Conditions: $m(Fe^0)$ = 0.025 g L^{-1}, $c(AO7)$ = 0.08 mmol L^{-1}, $c(Ox)$ = 1.0 mmol L^{-1}, pH = 2.5.

constant (min^{-1}). The constant k is calculated by the slope of a plot of $\ln(C_t/C_0)$ *versus* t and is summarized in Table 1.

$$C_t/C_0 = e^{-kt} \qquad (9)$$

3. Results and discussion

3.1. Effectiveness of the various activated peroxygens

Experiments were conducted to determine effectiveness of Fe^0 activated peroxygens on the removal of AO7 by changing initial pH of solution while keeping Fe^0 loading and peroxygens concentration constant. As shown in Fig. 1, degradation efficiency of AO7 decreased with the increasing pH value. About 20% of dye was decomposed in Fe^0/air system at pH = 2.5, while no measurable degradation was observed at other tested pH. Under acidic conditions, indirect oxidation of dye by strong oxidants generated by Fe^0 (eqn (4), (7) and (8)) was responsible for AO7 degradation besides the direct reductive decolorization on iron surface which results in the cleavage of the azo bonds of AO7 (eqn (10)).[13]

$$-N{=}N- + 2H^+ + 2e^- \rightarrow -NH + HN- \qquad (10)$$
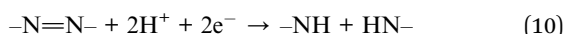
Mielczarski *et al.*[29] reported that iron oxide/hydroxide on the Fe^0 surface was thin at pH = 3.0, but mainly existed in the solution. Accumulation of iron oxide on the iron surface significantly affected the electron transfer between Fe^0 and oxygen (or dye) at pH > 4.0,[29] thus inhibiting the dye degradation. Among the three tested Fe^0-peroxygens systems, Fe^0/H_2O_2 system exhibited a better degradation efficiency at pH = 2.5,

with a constant rate of 0.16 min^{-1}, higher than those (0.12 min^{-1}) in two $SO_4^{\cdot-}$-based systems (Table 1). This can be ascribed to the higher oxidation capacity of $^{\cdot}OH$ than $SO_4^{\cdot-}$ at highly acidic pH. However, at higher pH (4.0 and 7.0), Fe^0/H_2O_2 system became inefficient towards dye degradation. At pH 7.0, no measurable degradation of dye occurred. In contrast, despite of reduction in reaction rates at pH 4.0 and 7.0, Fe^0/PMS and Fe^0/PS systems still led to a considerable degradation of AO7. Some researchers tried to explain it from the perspective of electron transfer mechanism.[18] They thought electron transfer from the iron surface to H_2O_2 undergoes an inner-sphere electron transfer process that is slower than outer-sphere electron transfer mechanism as supposed in Fe^0/PMS and Fe^0/PS systems. This proposed explanation is supported by Al-Shamsi *et al.*[18] and Rastogi *et al.*[30] who both observed that activated H_2O_2 system was less efficient to oxidize trichloroethylene (TCE) and polychlorinated biphenyls (PCBs) compared to the activated PS and PMS systems.

3.2. Effect of Fe^0 dosage

Effects of Fe^0 dosage (0.005, 0.025, 0.1 g L^{-1}) on dye degradation by four Fe^0-based systems were investigated. As seen in Fig. 2, without Fe^0, peroxygen itself can not directly oxidize dye within the examined time. Degradation efficiency of four tested systems all increased with increasing iron dosage. For example, about 90% of dye was degraded in Fe^0/H_2O_2 process at 10 min, while other reactions with relatively lower Fe^0 dosage (0.005, 0.025 g L^{-1}) needed longer reaction time of 20 and 30 min to achieve the comparable removal of dye, respectively. Increasing Fe^0 dosage from 0.005 to 0.1 g L^{-1} led to a 17.6, 3.7 and 10-fold increase in pseudo first-order rate constant in Fe^0, Fe^0/H_2O_2 and

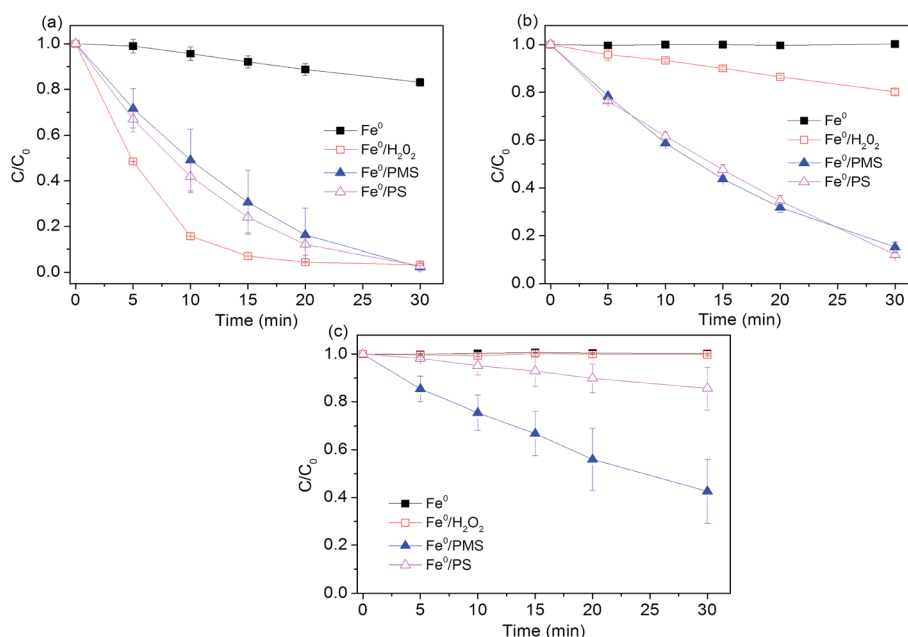**Fig. 1** Effect of pH value on AO7 degradation rates. (a) $pH_0 = 2.5$; (b) $pH_0 = 4.0$; (c) $pH_0 = 7.0$. Conditions: $c(AO7)_0 = 0.08$ mmol L^{-1}; $m(Fe^0)_0 = 0.025$ g L^{-1}; $c(Ox)_0 = 1$ mmol L^{-1}.

Fe^0/PS, respectively. Increase in total surface area and availability of more Fe^0 reactive sites should be responsible for the enhanced degradation of dye with increasing iron dosage.

3.3. Effects of peroxygens doses

The influence of peroxygens concentrations on the oxidation of AO7 with PS, PMS, H_2O_2 was studied at the ZVI dosage of

0.005 g. As expected, Fig. 3 shows that degradation rates of AO7 increased as PS and H_2O_2 dosage increased because of the enhanced generation of hydroxyl radical and sulfate radical as availability of their precursors (*i.e.* PS and H_2O_2) was increased. Briefly, the rate constant for dye degradation increased by a factor of 2.7 and 2.4 as concentration of H_2O_2 and PS increased from 0.5 to 1.5 mmol L^{-1}. As shown in Fig. 3b, the extent of AO7 degradation increased from 20% to 92.1% when
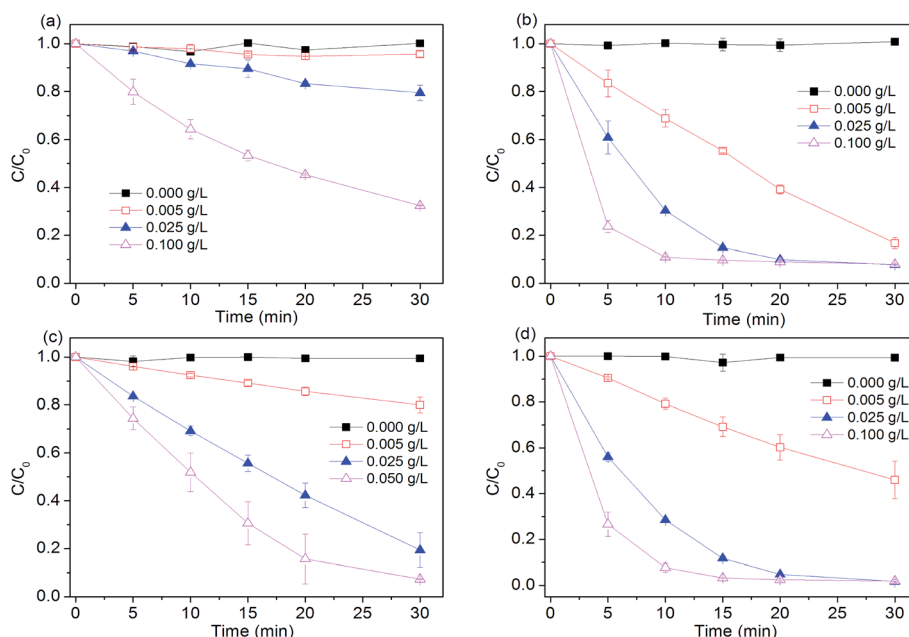

Fig. 2 Effect of Fe^0 dosage on AO7 removal in four systems. (a) Fe^0; (b) Fe^0/H_2O_2; (c) Fe^0/PMS; (d) Fe^0/PS. Conditions: $c(AO7)_0 = 0.08$ mmol L^{-1}; $c(Ox)_0 = 1$ mmol L^{-1}; $pH_0 = 2.5 \pm 0.2$.
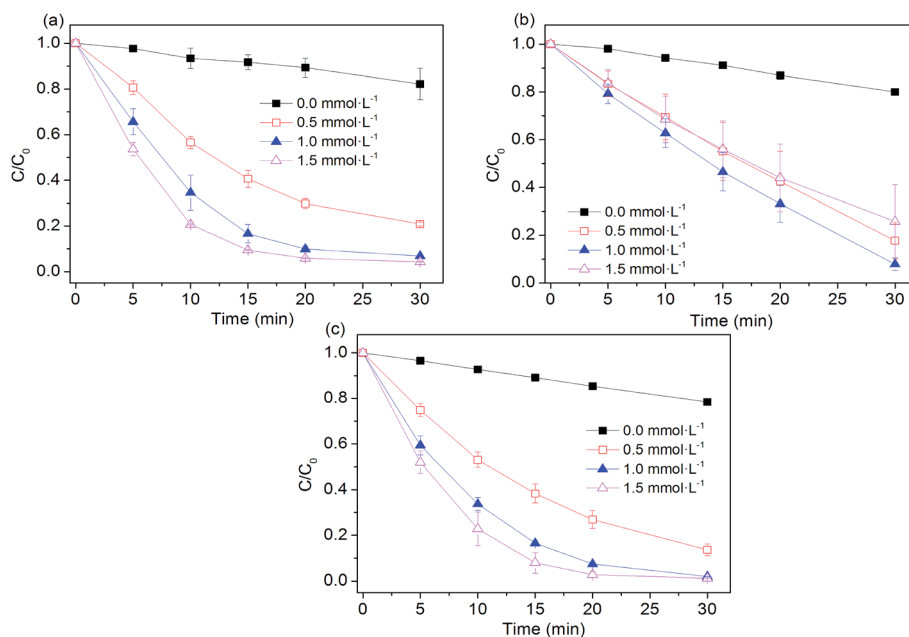
Fig. 3 Effect of peroxygens concentration on AO7 removal in four systems. (a) Fe^0/H_2O_2; (b) Fe^0/PMS; (c) Fe^0/PS. Conditions: $c(AO7)_0 = 0.08$ mmol L^{-1}; $m(Fe^0)_0 = 0.025$ g L^{-1}; $pH_0 = 2.5 \pm 0.2$.

PMS concentration increased from 0 to 1 mmol L^{-1} within 30 min. As PMS concentration was over 1 mmol L^{-1}, the removal of AO7 was decreased to about 70%. A similar trend was also observed during the oxidative degradation of bisphenol A (BPA) by UV activated PMS.[31] An excess of HSO_5^- may scavenge parts of $SO_4^{\bullet-}$ radicals and generate the less reactive $SO_5^{\bullet-}$ radicals (eqn (11)),[31,32] thus decreasing the degradation efficiency of dye pollutant.

$$HSO_5^- + SO_4^{\bullet-} \rightarrow HSO_4^- + SO_5^{\bullet-} \qquad (11)$$
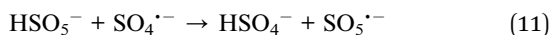
3.4. Effect of Cl^- concentration

Higher level of NaCl is one of the remarkable feature of textile wastewater, as large amount of NaCl (50–80 g L^{-1}) is frequently applied in dyeing processes in order to improve dye fixation and completion.[33] Our previous studies demonstrated that performance of $SO_4^{\bullet-}$-based advanced oxidation processes (SR-AOPs) is significantly affected by the presence of chloride.[34–43] Therefore, it is necessary to examine efficiencies of four Fe^0-based processes in the presence of chloride. As shown in Fig. 4, the NaCl in aqueous solution did not obviously affect the dye removal in the Fe^0 system. Effects of chloride on Fe^0-induced pollutant removal are quite complicated, depending on the nature of pollutants to be treated. For example, the presence of chloride can destroy the passive oxide layers and help to maintain efficiency of Fe^0 for nitrobenzene reduction.[44] However, Hwang et al.[45] reported that a higher concentration of NaCl (>3 g L^{-1}) had a significant inhibitory effect on nitrate reduction by Fe^0, although Fe^0 is known as a pitting and crevice corrosion promoter.[46]

In the Fe^0/H_2O_2 and Fe^0/PS systems, degradation rates of AO7 decreased in the presence of chloride. The negative effects of chloride ion on the efficiency of the Fe^0/H_2O_2 and Fe^0/PS systems may be explained by (Laat and Le 2006):[47] (1) the formation of Fe(III) or Fe(II)-chlorocomplexes ($FeCl^+$, $FeCl^{2+}$, $FeCl_2^+$) (eqn (12)–(14)) and (2) the scavenging effect of chloride ion for hydroxyl and sulfate radicals (eqn (15)–(18)). When chloride concentrations were less than 50 mmol L^{-1}, degradation efficiency of TCE,[48] p-nitrosodimethylaniline[49] and AO7 (ref. 50) by PS activation with Fe^0 was not significantly affected. In the presence of excess chloride, the reaction of $^\bullet OH$ or $SO_4^{\bullet-}$ with Cl^- leads to the formation of chlorine atoms ($Cl^\bullet$) ($E^0(Cl^\bullet/Cl^-) = 2.41$ V vs. NHE) and of dichloride anion radicals ($Cl_2^{\bullet-}$) ($E^0(Cl_2^{\bullet-}/2Cl^-) = 2.09$ V vs. NHE).[51] $Cl^\bullet/Cl_2^{\bullet-}$ can oxidize H_2O_2 and Fe(II) and but are less reactive with organic solutes than either $^\bullet OH$ or $SO_4^{\bullet-}$. It should be noted that dye degradation was significantly accelerated in $Fe^0/PMS/Cl^-$ systems. For example, at $[Cl^-] = 400$ mmol L^{-1}, k increased 15 times higher than that in the absence of chloride. Our previous investigations found that PMS, rather than H_2O_2 and PS, could directly react with Cl^- to produce HOCl and Cl_2 (eqn (19) and (20)),[37–43,51] enhancing the dye bleaching rate.
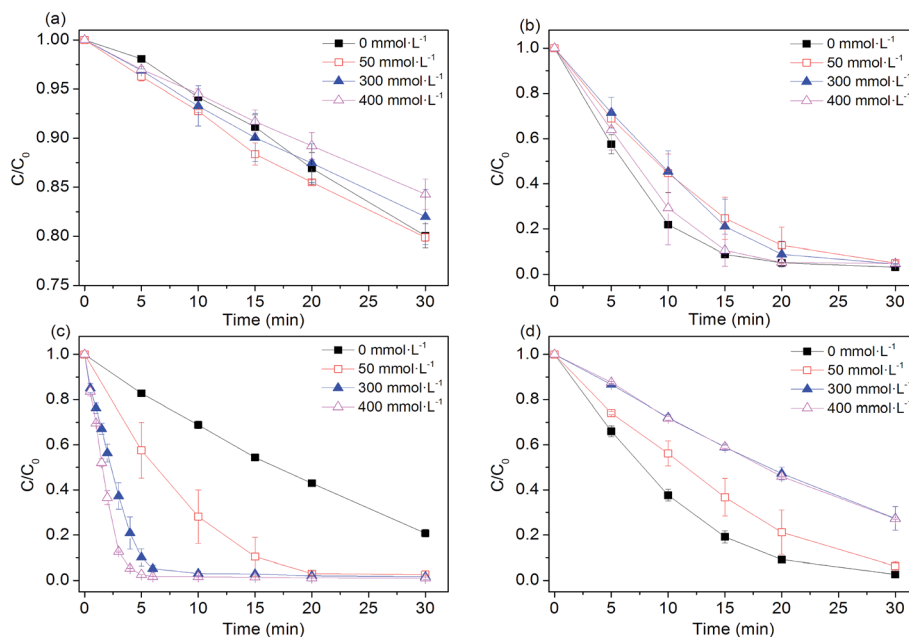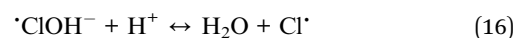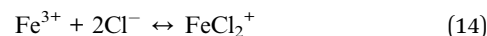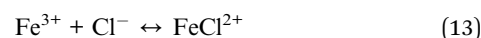
$$Fe^{2+} + Cl^- \leftrightarrow FeCl^+ \qquad (12)$$

$$Fe^{3+} + Cl^- \leftrightarrow FeCl^{2+} \qquad (13)$$

$$Fe^{3+} + 2Cl^- \leftrightarrow FeCl_2^+ \qquad (14)$$

$$Cl^- + {}^\bullet OH \leftrightarrow {}^\bullet ClOH^- \qquad (15)$$

$${}^\bullet ClOH^- + H^+ \leftrightarrow H_2O + Cl^\bullet \qquad (16)$$

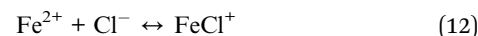$$Cl^- + SO_4^{\bullet-} \leftrightarrow Cl^\bullet + SO_4^{2-} \qquad (17)$$

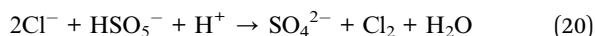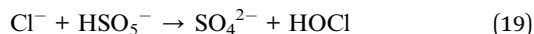**Fig. 4** Effect of chloride ions on AO7 degradation rates. (a) Fe^0; (b) Fe^0/H_2O_2; (c) Fe^0/PMS; (d) Fe^0/PS. Conditions: $c(AO7)_0 = 0.08$ mmol L^{-1}; $m(Fe^0)_0 = 0.025$ g L^{-1}; $c(Ox)_0 = 1$ mmol L^{-1}; $pH_0 = 2.5 \pm 0.2$.

$$Cl^\bullet + Cl^- \leftrightarrow Cl_2^{\bullet-} \qquad (18)$$

$$Cl^- + HSO_5^- \rightarrow SO_4^{2-} + HOCl \qquad (19)$$

$$2Cl^- + HSO_5^- + H^+ \rightarrow SO_4^{2-} + Cl_2 + H_2O \qquad (20)$$
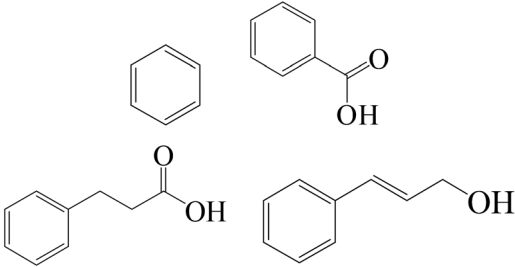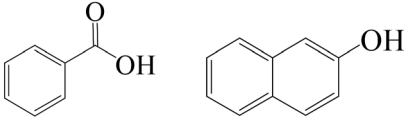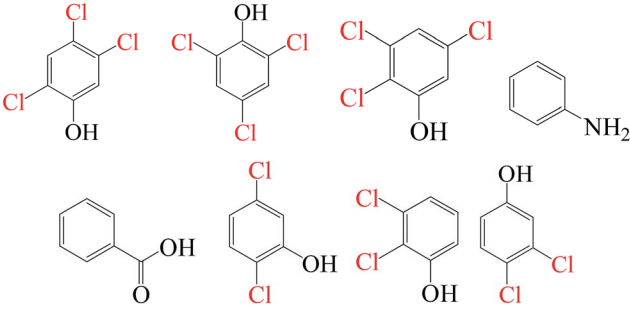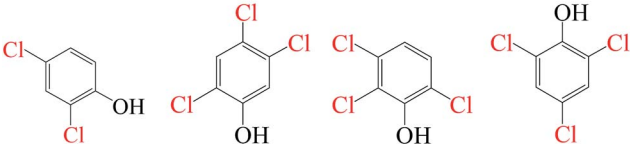
3.5. AO7 mineralization and byproducts identification

As evidenced in the previous studies, chlorinated organic intermediates would be generated when amounts of chloride are present in SR-AOPs. Therefore, it is necessary to identify the reaction byproducts and evaluate the mineralization, besides testing degradation rates. GC-MS data (Fig. S1–S18,† Table 2) show that some chlorinated compounds were produced in SR-AOPs. Seven chlorinated phenols, including 2,3,6-trichlorophenol, 2,4,5-trichlorophenol, 2,4,6-trichlorophenol, 3,4-dichlorophenol, 2,5-dichlorophenol, 2,3-dichlorophenol, 2,4-dichlorophenol, were identified in Fe^0/PMS/Cl$^-$ system, whereas only three chlorophenols like 2,4,5-trichlorophenol, 2,4,6-trichlorophenol, 2,3,5-trichlorophenol were detected in Fe^0/PS/Cl$^-$ system. According to the known Material Safety Data Sheet (MSDS) of pure chemical, acute toxicity, expressed as rat

Lethal Dose, 50% (LD50), are 820 mg kg^{-1} for 2,4,5-trichlorophenol, 820 mg kg^{-1} for 2,4,6-trichlorophenol, 1685 mg kg^{-1} for 3,4-dichlorophenol, 2376 mg kg^{-1} for 2,3-dichlorophenol and 47 mg kg^{-1} for 2,4-dichlorophenol, respectively, much greater than 3418 mg kg^{-1} for their parent compound, AO7. This indicates that AO7 was transformed to more toxic and recalcitrant organic byproducts although AO7 itself has been efficiently degraded in Fe^0-based oxidation systems.

Fig. 5 illustrates that 15.1% of AO7 could be mineralized without the addition of chloride after 30 min oxidation in Fe^0/H$_2$O$_2$ system. The extent of mineralization in descending order is Fe^0/H$_2$O$_2$ > Fe^0/PS > Fe^0/PMS > Fe^0 (Fig. 5a). In the presence of chloride, TOC removal were dramatically decreased in four systems (Fig. 5b). In particular, no measurable TOC removal were observed in Fe^0/PMS system, in sharp contrast to its rapid degradation rate as shown in Fig. 4. In combination with the GC-MS data, it is evident that AO7 in Fe^0/PMS/Cl$^-$ system was only converted to some chlorinated byproducts, although it was rapidly bleached. In general, extents of mineralization in these tested systems were not satisfactory. It is probably because (1) AO7 is just degraded via a chromophore cleavage, as evidenced by GC-MS; (2) Fe^0, as a strong reductant, may continuously

Table 2 The transformation products during oxidation of AO7 in Fe^0-peroxygens systems

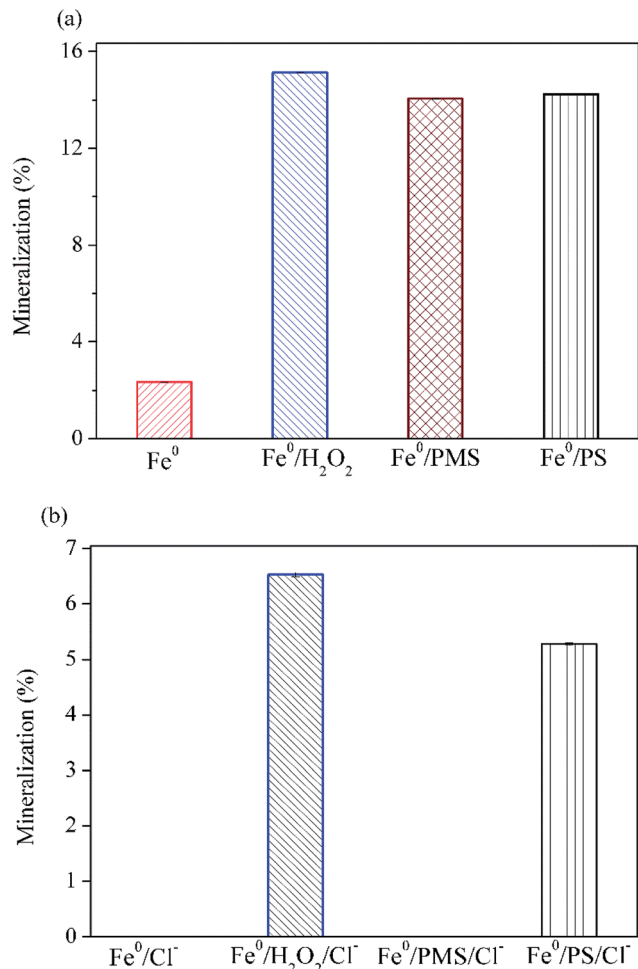| Systems	Identified by products
Fe^0/Cl$^-$	
Fe^0/H$_2$O$_2$/Cl$^-$	
Fe^0/PS/Cl$^-$	
Fe^0/PMS/Cl$^-$	

(a)

(b)

Fig. 5 Variation of mineralization of AO7 with different peroxygens after 30 min. (a) Without Cl^-; (b) with Cl^-. Conditions: $c(AO7)_0 = 0.08$ mmol L^{-1}; $m(Fe^0)_0 = 0.025$ g L^{-1}; $c(Ox)_0 = 1$ mmol L^{-1}; $pH_0 = 2.5 \pm 0.2$; $c(NaCl)_0 = 50$ mmol L^{-1} (if any).

consume highly reactive species which are critical for a complete mineralization of organic pollutant. The development of processes combining Fe-based peroxygens oxidation systems with further biological methods is a possible route to improve the removal of recalcitrant degradation intermediates.

3.6. Mechanism discussion

Under the present experimental conditions, two major mechanisms govern the removal process of dye: (1) reduction and (2) degradation. Fe^0 undergoes a couples of corrosion reactions in acidic solution, accompanying with reduction of O_2 or pollutants on its surface. Azo dye reduction is thought to involve a two-step process.[52] Initially, nascent hydrogen is generated after the oxidation of Fe^0. The newly formed Fe^{2+} on the Fe^0 surface enables the azo group of AO7 catalytically hydrogenated to form short-lived hydrazo intermediates, followed by a further hydrogenation of the unstable transition products to form stable aromatic amines.

In addition to dye pollutant, O_2 can be directly reduced by Fe^0 powder to generate H_2O_2 (eqn (2)), providing the reactants

for the Fenton reaction yielding $^\bullet$OH radical. A faster iron redox cycle at the iron surface takes place through a rapid reduction of Fe^{3+} to Fe^{2+} by Fe^0. The kinetic rates of iron corrosion are dependent upon the intrinsic reactivity of the selected Fe material and other environmental factors, such redox conditions and pH.[53] At neutral pH, a thick layer of iron oxides, maghemite or lepidocrocite, is formed as a result of hydrolysis, precipitation and transformation of Fe^{3+}, thereby diminishing the reactivity of Fe^0.

In the presence of peroxygens, $^\bullet$OH or $SO_4^{\bullet-}$ is produced from the catalytic decomposition of H_2O_2, PS and PMS by Fe^0 and/or Fe^{2+}. Surface-catalyzed Fe^{2+} oxidation may play an important role in peroxygens activation. Keenan and Sedlak[12] found that accelerated Fe^{2+} oxidation in the presence of Fe surface significantly contributed to the enhanced HCHO yields from oxidation of CH_3OH at pH > 6.0. Therefore, it is reasonably expected that surface-catalyzed Fe^{2+} reactions with peroxygens vary with the homogeneous reactions and deserves in-depth investigations in future.

4. Conclusions

In this work, commercially available Fe^0 powder was used to activate three common peroxygens (H_2O_2, PS and PMS) for the degradation of a model hazardous azo dye (*i.e.*, AO7). Experimental data indicate Fe^0 was an effective activator for peroxygens to treat azo dye at acidic pH. The highest AO7 oxidation and mineralization were achieved in Fe^0 activated H_2O_2 system at pH 2.5. However, the ability of Fe^0 activated H_2O_2 system to oxidize AO7 was less than those of Fe^0/PS and Fe^0/PMS systems at pH $\geq$ 4.0. Increasing iron dosage and peroxygens concentration favored a rapid degradation of AO7 in Fe^0/PS and Fe^0/H_2O_2 systems. Addition of chloride could greatly inhibit dye removal in Fe^0/H_2O_2 and Fe^0/PS systems, whereas dye degradation was accelerated in Fe^0/PMS system. In contrast, no measurable mineralization of AO7 in Fe^0/PMS/Cl^- system was observed. Some refractory chlorinated phenols, such as 2,3,6-trichlorophenol, 2,4,5-trichlorophenol, 2,3,5-trichlorophenol, 2,4,6-trichlorophenol, 3,4-dichlorophenol, 2,5-dichlorophenol, 2,3-dichlorophenol and 2,4-dichlorophenol were identified by GC-MS. In conclusion, Fe^0/H_2O_2 system is recommended to treat acidic and saline wastewater, while Fe^0/PS and Fe^0/PMS processes are more suitable for treatment of low salinity wastewater.

References

1 H. Zollinger, *Colour Chemistry-Synthesis*, 1987.

2 Z. H. Wang, W. H. Ma, C. C. Chen and J. C. Zhao, *J. Hazard. Mater.*, 2009, **168**, 1246.

3 H. L. Lien and W. X. Zhang, *Appl. Catal., B*, 2007, **77**, 110.

4 G. V. Lowry and K. W. Johnson, *Environ. Sci. Technol.*, 2004, **38**, 5208.

5 S. Choe, Y. Y. Chang, K. Y. Hwang and J. Khim, *Chemosphere*, 2000, **41**, 1307.

6 J. Cao, L. P. Wei, Q. G. Huang, L. S. Wang and S. K. Han, *Chemosphere*, 1999, **38**, 565.

7 G. Roy, P. D. Donato, T. Görner and O. Barres, *Water Res.*, 2003, **37**, 4954.

8 S. Nam and P. G. Tratnyek, *Water Res.*, 2000, **34**, 1837.

9 F. S. Freyria, B. Bonelli, R. Sethi, M. Armandi, E. Belluso and E. Garrone, *J. Phys. Chem. C*, 2011, **115**, 24143.

10 Y. He, J. F. Gao, F. Q. Feng, C. Liu, Y. Z. Peng and S. Y. Wang, *Chem. Eng. J.*, 2012, **179**, 8.

11 Y. Yuan, H. Q. Li, B. Lai, P. Yang, M. Gou, Y. X. Zhou and G. Z. Sun, *Ind. Eng. Chem. Res.*, 2014, **53**, 2605.

12 C. R. Keenan and D. L. Sedlak, *Environ. Sci. Technol.*, 2008, **42**, 1262.

13 S. H. Chang, K. S. Wang, S. J. Chao, T. H. Peng and L. C. Huang, *J. Hazard. Mater.*, 2009, **166**, 1127.

14 O. X. Leupin and S. J. Hug, *Water Res.*, 2005, **39**, 1729.

15 C. E. Noradoun and I. F. Cheng, *Environ. Sci. Technol.*, 2005, **39**, 7158.

16 S. H. Joo, A. J. Feitz, D. L. Sedlak and T. D. Waite, *Environ. Sci. Technol.*, 2005, **39**, 1263.

17 C. J. Liao, T. L. Chung, W. L. Chen and S. L. Kuo, *J. Mol. Catal. A: Chem.*, 2007, **265**, 189.

18 M. A. Al-Shamsi, N. R. Thomson and S. P. Forsey, *Chem. Eng. J.*, 2013, **232**, 555.

19 J. Y. Zhao, Y. B. Zhang, X. Quan and S. Chen, *Sep. Purif. Technol.*, 2010, **71**, 302.

20 S. Y. Oh, S. G. Kang and P. C. Chiu, *Sci. Total Environ.*, 2010, **408**, 3464.

21 C. J. Liang and M. C. Lai, *Environ. Eng. Sci.*, 2008, **25**, 1071.

22 Z. H. Wang, R. T. Bush, L. A. Sullivan and J. S. Liu, *Environ. Sci. Technol.*, 2013, **47**, 6486.

23 Z. H. Wang, R. T. Bush, L. A. Sullivan, C. C. Chen and J. S. Liu, *Environ. Sci. Technol.*, 2014, **48**, 3978.

24 I. Hussain, Y. Q. Zhang and S. B. Huang, *RSC Adv.*, 2014, **4**, 3502.

25 X. X. Jiang, Y. L. Wu, P. Wang, H. J. Li and W. B. Dong, *Environ. Sci. Pollut. Res.*, 2013, **20**, 4947.

26 S. Rodriguez, L. Vasquez, A. Romero and A. Santos, *Ind. Eng. Chem. Res.*, 2014, **53**, 12288.

27 Y. X. Wang, H. Q. Sun, X. G. Duan, H. M. Ang, M. O. Tadé and S. B. Wang, *Appl. Catal., B*, 2015, **172–173**, 73.

28 H. Y. Shu, M. C. Chang and C. C. Chang, *J. Hazard. Mater.*, 2009, **167**, 1178.

29 J. A. Mielczarski, G. M. Atenas and E. Mielcazrski, *Appl. Catal., B*, 2005, **56**, 289.

30 A. Rastogi, S. R. Al-Abed and D. D. Dionysiou, *Appl. Catal., B*, 2009, **85**, 171.

31 J. Sharma, I. M. Mishra, D. D. Dionysiou and V. Kumar, *Chem. Eng. J.*, 2015, **276**, 193.

32 P. Maruthamuthu and P. Neta, *J. Phys. Chem.*, 1977, **81**, 937.

33 Washington and DC, Environmental Protection Agency, 1997.

34 S. N. Ramjaun, R. X. Yuan, Z. H. Wang and J. S. Liu, *Electrochim. Acta*, 2011, **58**, 364.

35 R. X. Yuan, S. N. Ramjaun, Z. H. Wang and J. S. Liu, *Chem. Eng. J.*, 2012, **192**, 171.

36 R. X. Yuan, S. N. Ramjaun, Z. H. Wang and J. S. Liu, *Chem. Eng. J.*, 2012, **209**, 38.

37 C. L. Fang, D. X. Xiao, W. Q. Liu, X. Y. Lou, J. Zhou, Z. H. Wang and J. S. Liu, *Chemosphere*, 2016, **144**, 2415.

38 J. Zhou, J. H. Xiao, D. X. Xiao, Y. G. Guo, C. L. Fang, X. Y. Lou, Z. H. Wang and J. S. Liu, *Chemosphere*, 2015, **134**, 446.

39 R. X. Yuan, Z. H. Wang, Y. Hu, B. H. Wang and S. M. Gao, *Chemosphere*, 2014, **109**, 106.

40 X. Y. Lou, Y. G. Guo, D. X. Xiao, Z. H. Wang and J. S. Liu, *Environ. Sci. Pollut. Res.*, 2013, **20**, 6317.

41 L. Xu, R. X. Yuan, Y. G. Guo, D. X. Xiao, Y. Cao, Z. H. Wang and J. S. Liu, *Chem. Eng. J.*, 2013, **217**, 169.

42 Z. H. Wang, R. X. Yuan, Y. G. Guo, L. Xu and J. S. Liu, *J. Hazard. Mater.*, 2011, **190**, 1083.

43 R. X. Yuan, S. N. Ramjaun, Z. H. Wang and J. S. Liu, *J. Hazard. Mater.*, 2011, **196**, 173.

44 W. Z. Yin, J. H. Wu, P. Li, X. D. Wang, N. W. Zhu, P. X. Wu and B. Yang, *Chem. Eng. J.*, 2012, **184**, 198.

45 Y. Hwang, D. Kim and H. S. Shin, *Environ. Technol.*, 2015, **36**, 1178.

46 T. X. Liu, X. M. Li and T. D. Waite, *Environ. Sci. Technol.*, 2013, **47**, 7350.

47 J. D. Laat and T. G. Le, *Appl. Catal., B*, 2006, **66**, 137.

48 C. J. Liang, Z. Wang and N. Mohanty, *Environ. Sci. Technol.*, 2006, **370**, 271.

49 L. R. Bennedsen, J. Muff and E. G. Sogaard, *Chemosphere*, 2012, **86**, 1092.

50 H. Li, J. Wan, Y. Ma, Y. Wang and Z. Guan, *RSC Adv.*, 2015, **5**, 99935.

51 S. N. Ramjaun, Z. H. Wang, R. X. Yuan and J. S. Liu, *J. Environ. Chem. Eng.*, 2015, **3**, 1648.

52 L. J. Matheson and P. G. Tratnyek, *Environ. Sci. Technol.*, 1994, **28**, 2045.

53 X. Sun, T. Kurokawa, M. Suzuki, M. Takagi and Y. Kawase, *J. Environ. Sci. Health, Part A: Toxic/Hazard. Subst. Environ. Eng.*, 2015, **50**, 1057.